

PROTON DAMAGE ANNEALING KINETICS IN SILICON SOLAR CELLS  
 W. E. Horne, I. Arimura and A. C. Day  
 The Boeing Aerospace Company, Seattle, Washington 98124

N82 22720

Proton damage annealing has been postulated as a method for prolonging the life of solar power systems in space. This paper describes a study of such damage annealing. The objectives of the study were to 1) minimize variables and examine fundamental characteristics of proton damage annealing, 2) to make preliminary evaluation of the usefulness of annealing for prolonging space missions, 3) to make a preliminary determination of optimum annealing conditions, and 4) to provide a data base for planning more detailed research programs.

A preliminary analytical model has been developed to describe the annealing of proton damage as a function of time and temperature in silicon solar cells. The analytical work is supported by data from detailed isochronal and isothermal annealing experiments on 2-Ω-cm N/P silicon solar cells after irradiation to various fluences of 1.5 MeV protons.

The data indicate that several defect species are created in silicon during the irradiate-anneal process and that each species anneals with its own characteristic time-temperature kinetics. This observation is in general agreement with those of other workers for high energy electron and neutron damage annealing. The relative amount of each species of defect appears to be a function of either the silicon starting material, i.e., low or high dislocation density, or the impurity concentrations such as oxygen, phosphorous, and boron in the silicon. It is found that the annealing process for the cells studied can be described by a model which considers that at room temperature the defects consist mainly of vacancy clusters. In the temperature range 100 to 150°C these clusters begin to break up and release vacancies. Between 150 and 200°C, these released vacancies diffuse throughout the silicon and either pair with interstitial silicon atoms and disappear (anneal) or pair with other impurity atoms creating new defect species (reverse anneal). At still higher temperatures these newly created defects are disassociated and eventually annealed. This model is supported by the isochronal annealing data of figure 1. The model can be expressed analytically by the following equations:

$$N_v = N_v^0 e^{-\frac{T}{\tau_v}} \quad (1)$$

$$N_{1v} = \frac{N_1}{N_1 + N_1 + N_2} \left( \frac{\tau_{1v}}{\tau_v - \tau_{1v}} \right) N_v^0 \left[ e^{-T/\tau_v} - e^{-T/\tau_{1v}} \right] \quad (2)$$

$$N_{2v} = \frac{N_2}{N_1 + N_1 + N_2} \left( \frac{\tau_{2v}}{\tau_v - \tau_{2v}} \right) N_v^0 \left[ e^{-T/\tau_v} - e^{-T/\tau_{2v}} \right] \quad (3)$$

where  $N_V^0$  is the number of vacancy clusters after irradiation,  $N_V$  is the number of vacancy clusters as a function of time,  $N_{1V}$  is the number of impurity number 1-vacancy complexes as a function of time,  $N_{2V}$  is the number of impurity number 2-vacancy complexes as a function of time,  $\tau_V$ ,  $\tau_{1V}$ ,  $\tau_{2V}$  are the annealing time constants for vacancy clusters, impurity number 1-vacancy, and impurity number 2-vacancy respectively, and  $N_1$ ,  $N_1$ ,  $N_2$  are the number of interstitials, impurity number 1, and impurity number 2 atoms respectively. Then the degradation in short circuit current can be expressed by:

$$\frac{1}{I_{sc}} - \frac{1}{I_{sc0}} \approx K_V N_V + K_{1V} N_{1V} + K_{2V} N_{2V} \quad (4)$$

$$F = \frac{\frac{1}{I_{sc}} - \frac{1}{I_{sc0}}}{\frac{1}{I_{sc\phi}} - \frac{1}{I_{sc0}}} \approx \frac{I_V N_V + K_{1V} N_{1V} + K_{2V} N_{2V}}{K_V N_V^0} \quad (5)$$

$$F = e^{-\frac{t}{\tau_V}} \left\{ 1 + \frac{1}{K_V(N_1+N_1+N_2)} \left[ \frac{N_1 K_{1V} \tau_{1V}}{\tau_V - \tau_{1V}} \left( 1 - e^{-t \left( \frac{1}{\tau_{1V}} - \frac{1}{\tau_V} \right)} \right) + \frac{N_2 K_{2V} \tau_{2V}}{\tau_V - \tau_{2V}} \left( 1 - e^{-t \left( \frac{1}{\tau_{2V}} - \frac{1}{\tau_V} \right)} \right) \right] \right\} \quad (6)$$

where  $F$  is the fraction of defects remaining,  $I_{sc}$  is the short circuit current as a function of time,  $I_{sc0}$  is the short circuit current before irradiation, and  $I_{sc\phi}$  is the short circuit current immediately after irradiation. That the equation (6) can qualitatively describe the annealing process is illustrated by the isothermal annealing data of figures 2, 3, 4, and 5 compared to a calculated curve using equation (6). It is hypothesized that impurity number 1 is oxygen and impurity number 2 is the dopant impurity boron. This hypothesis is supported by comparison of annealing temperatures for each stage to that of neutron annealing data where the defects have been more positively identified.

Figures 6 and 7 show the degree to which the power output of the proton damaged cells can be restored. From these data it appears advantageous to anneal at as high a temperature as possible. It was further observed that the cells annealed after  $3 \times 10^{11}$  p/cm<sup>2</sup> annealed more rapidly and more completely than those annealed after  $3 \times 10^{12}$  p/cm<sup>2</sup>.

It is further interesting to note that, although the cells had relatively uniform electrical characteristics and degraded in a uniform manner as illustrated in figure 8, the annealing response showed a wide degree of scatter both in recovery times and in degree of recovery. This suggests that the annealing process is governed by parameters which do not strongly affect either initial cell performance or cell radiation resistance. If this is true and the factors yielding faster and more complete recovery can be identified then cells optimized for annealing should be possible.

Conclusions that can be drawn are that 1) the annealing can be effective in restoring the performance of proton damaged cells and 2) factors such as silicon starting material, dopant materials, proton energy spectrum, damage level at which anneals are performed, temperature/time profiles, and solar cell junction designs should be considered in order to optimize annealing conditions.

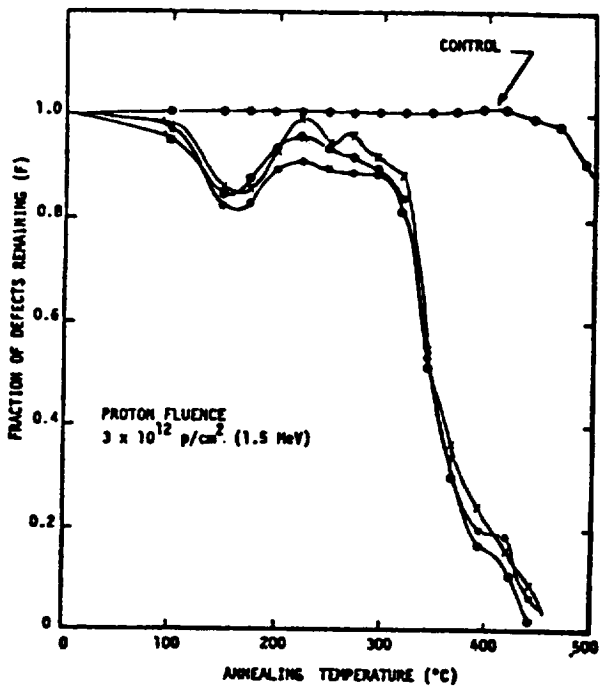


Figure 1. Isochronal Annealing of Proton Damage

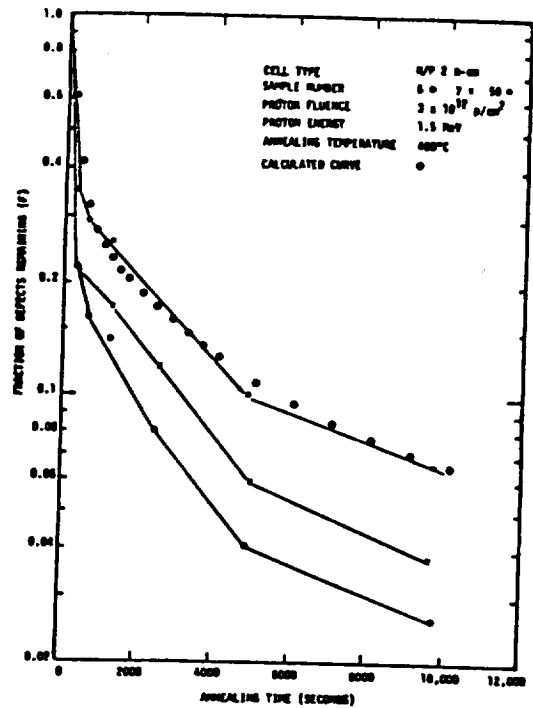


Figure 2. Isothermal Annealing of  $3 \times 10^{12}$  p/cm<sup>2</sup> Proton Damage at 400°C

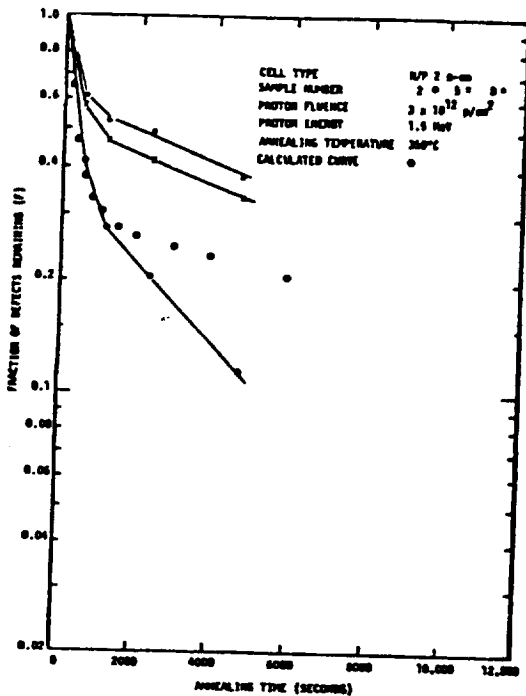


Figure 3. Isothermal Annealing of  $3 \times 10^{12}$  p/cm<sup>2</sup> Proton Damage at 350°C

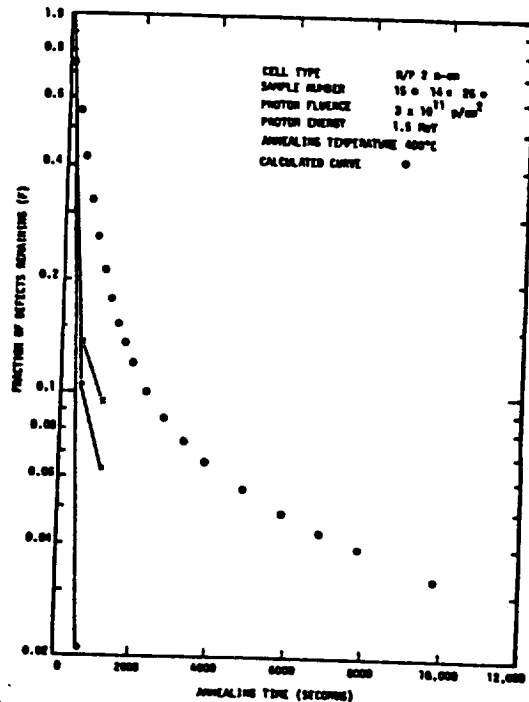


Figure 4. Isothermal Annealing of  $3 \times 10^{11}$  p/cm<sup>2</sup> Proton Damage at 400°C

ORIGINAL PAGE IS OF POOR QUALITY

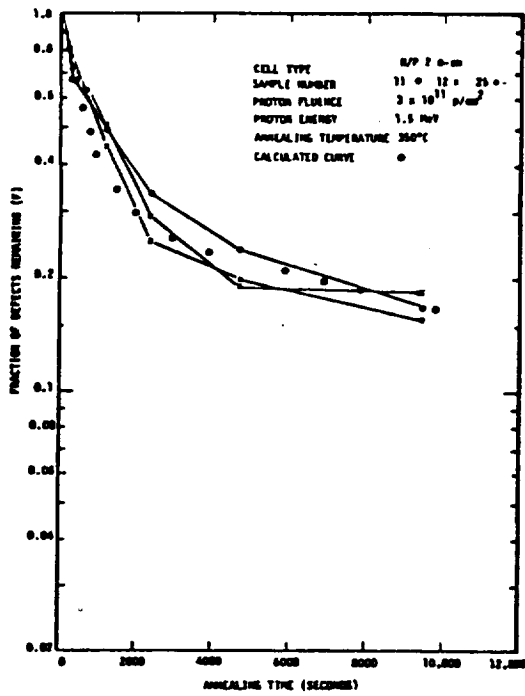


Figure 5. Isothermal Annealing of  $3 \times 10^{11}$  p/cm<sup>2</sup> Proton Damage at 350°C

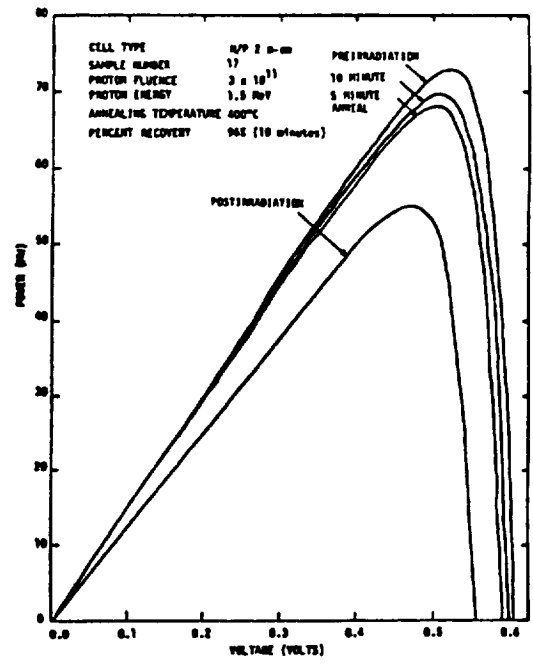


Figure 6. Recovery of Solar Cell Power After  $3 \times 10^{11}$  p/cm<sup>2</sup> at 400°C

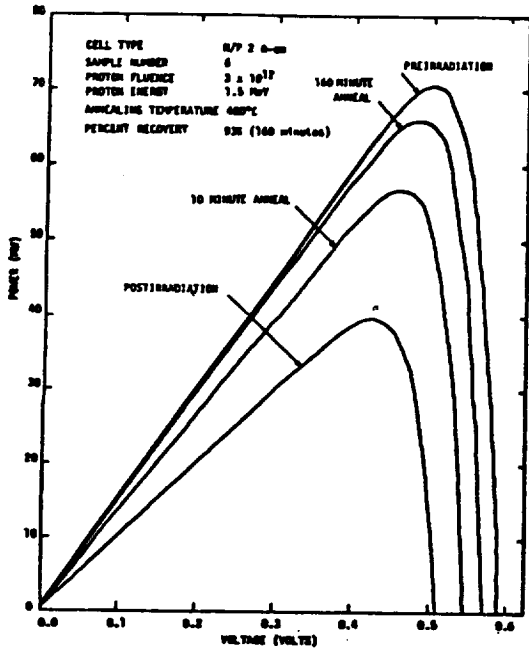


Figure 7. Recovery of Solar Cell Power After  $3 \times 10^{12}$  p/cm<sup>2</sup> at 400°C

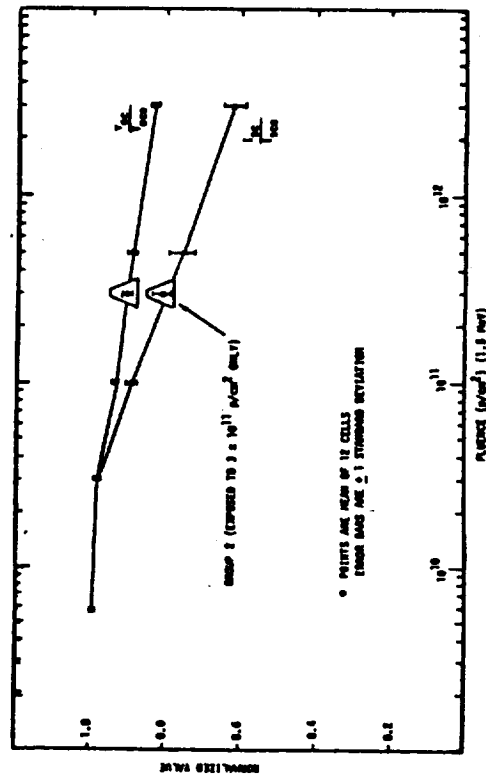


Figure 8. Normalize Degradation of 2 Groups of 12 Cells Each N/P 2-ohm Cells Exposed to 1.5 MeV Protons

ORIGINAL PAGE IS OF POOR QUALITY